

A new coupling algorithm for density-driven flow in porous media

Philippe Ackerer

Institut de Mécanique des Fluides et des Solides, UMR 7507, Strasbourg, France

Anis Younès

Laboratoire de Génie Industriel, Université la Réunion, St. Denis, France

Martial Mancip

Projet Estime, INRIA Rocquencourt, Le Chesnay, France

Received 15 January 2004; accepted 27 May 2004; published 26 June 2004.

[1] We consider the numerical solution of coupled fluid flow and heat or mass transport in porous media. The aim of this work is to provide some new mathematical development and algorithm to reduce the CPU costs of the solution of these strongly non-linear coupled equations widely used in geosciences and environmental sciences, without loss of accuracy. Usually, the flow equation is solved first. We show that, by solving the transport equation first, the CPU time can be significantly reduced. This new algorithm is not dependent on the numerical scheme and is quite easy to implement in a numerical code. The accuracy of this new way of coupling flow and transport equations is evaluated with 2D and 3D numerical tests. *INDEX TERMS*: 3210 Mathematical Geophysics: Modeling; 3230 Mathematical Geophysics: Numerical solutions; 3299 Mathematical Geophysics: General or miscellaneous. **Citation**: Ackerer, P., A. Younès, and M. Mancip (2004), A new coupling algorithm for density-driven flow in porous media, *Geophys. Res. Lett.*, 31, L12506, doi:10.1029/2004GL019496.

1. Introduction

[2] In this work, we tackle the solution of coupled fluid flow and heat or mass transport in porous media. For these problems, the fluid properties (density, viscosity) are dependent upon temperature or concentration. Therefore, fluid flow processes occurring in porous media are described by coupled nonlinear systems of partial differential equations (PDEs). Because of this nonlinearity, there are hardly any analytical solutions and we resort to numerical models to understand and predict solute and/or heat distribution in the domain.

[3] A lot of numerical codes have been developed and we present here a new strategy for solving this system of coupled equations. This strategy can be applied whatever the numerical method used to solve each equation. This strategy will be used to simulate a 2D standard widely used benchmark (Elder test case [Elder, 1966]) and a 3D experiment called the saltpool experiment [Oswald, 1998; Oswald and Kinzelbach, 2004].

2. Mathematical Models

[4] The more common mathematical models of coupled fluid flow and heat or mass transport in porous media are

based on the work of Bear [1972]. The proposed model has been widely discussed by Hassanizadeh and Leijnse [1988] and Diersch and Kolditz [1998, 2002] among others.

[5] The system of flow equations with varying density and viscosity is obtained from the mass conservation of the fluid,

$$\frac{\partial(\phi\rho)}{\partial t} + \nabla \cdot (\rho\mathbf{q}) = \rho Q, \quad (1)$$

where ϕ is the porosity, ρ the mass density of the fluid, \mathbf{q} the specific discharge (Darcy velocity) and Q the sink/source term, and the generalized Darcy's law,

$$\mathbf{q} = -\frac{\mathbf{k}}{\mu}(\nabla P + \rho\mathbf{g}\nabla z), \quad (2)$$

where μ is the dynamic viscosity of the fluid, \mathbf{k} the permeability tensor of the porous medium, P the fluid pressure and \mathbf{g} the gravity acceleration.

[6] Usual assumptions concerning the physical processes of heat or solute transport in saturated porous media leads to the same mathematical model, a convection–dispersion partial differential equation:

$$\frac{\partial(c\rho\omega)}{\partial t} + \nabla \cdot (\mathbf{q}\rho\omega) - \nabla \cdot (\rho\mathbf{D}\nabla\omega) = Q\omega_s, \quad (3)$$

where ω is the state variable (temperature or solute mass fraction), ω_s is the state variable at sources, c the cumulative term (porosity for solute, specific heat capacity for temperature), and \mathbf{D} is the dispersion/diffusion tensor where thermal conductivities of the solid and the fluid phases have to be added for heat transport. Detailed presentation of the transport models and their underlying assumptions are given in the review paper of Diersch and Kolditz [2002].

[7] Equations of flow, heat and mass transfer are coupled by the equations of state which gives the fluid density and viscosity as functions of mass fraction and/or temperature. Often the fluid density equation is expressed as a linear function of the mass fraction and/or temperature. More complicated equations of state are used for viscosity [Diersch and Kolditz, 2002].

[8] Different assumptions are usually made to reduce the nonlinear relationships between the PDEs [Kolditz et al., 1998; Holzbecher, 1998]. The assumption stated by Bear

[1972] has been found efficient without significant loss of accuracy [Ackerer et al., 2000; Younès, 2003].

[9] For transport problems, the density term in equation (3) may also be neglected [Younès et al., 1999].

3. A New Sequential Coupling Algorithm

[10] Considering the solid matrix rigid and immobile, the porosity only a function of pressure P , and using $h = \frac{P}{\rho_0 g} + z$, $S = \rho_0 g S_p$ and $\mathbf{K} = \frac{\rho_0 g}{\mu} \mathbf{k}$, the combination of the generalized Darcy's law (2) and the mass balance equation (1) of the fluid, leads to:

$$\rho S \frac{\partial h}{\partial t} + c \frac{\partial \rho}{\partial \omega} \frac{\partial \omega}{\partial t} + \nabla \cdot (\rho \mathbf{q}) = \rho Q, \mathbf{q} = -\mathbf{K} \left(\nabla h + \frac{\rho - \rho_0}{\rho_0} \nabla z \right). \quad (4)$$

where S_p is the specific storage coefficient [Huyakorn et al., 1987].

[11] Usually, the transport equation is written in the following form, using equation (1):

$$c \frac{\partial \omega}{\partial t} + \mathbf{q} \cdot \nabla \omega - \nabla \cdot (\mathbf{D} \cdot \nabla \omega) = Q(\omega_s - \omega) \quad (5)$$

and the three PDEs are linearized with a Picard scheme (fixed point) and solved iteratively as follows:

$$\left. \begin{array}{l} \text{Step 1 : } S \frac{h^{n+1,k+1} - h^n}{\Delta t} + \nabla \cdot \left(-\mathbf{K} \left(\nabla h^{n+1,k+1} + \frac{\rho^{n+1,k} - \rho_0}{\rho_0} \nabla z \right) \right) = Q \frac{c}{\rho} \frac{\partial \rho}{\partial \omega} \frac{\omega^{n+1,k} - \omega^n}{\Delta t} \\ \text{Step 2 : } \mathbf{q}^{n+1,k*} = -\mathbf{K} \left(\nabla h^{n+1,k+1} + \frac{\rho^{n+1,k} - \rho_0}{\rho_0} \nabla z \right) \\ \text{Step 3 : } c \frac{\omega^{n+1,k+1} - \omega^n}{\Delta t} + \mathbf{q}^{n+1,k*} \cdot \nabla \omega^{n+1,k+1} - \nabla \cdot (\mathbf{D}^{n+1,k*} \cdot \nabla \omega^{n+1,k+1}) = Q(\omega_s - \omega^{n+1,k+1}) \\ \text{Step 4 : } \rho^{n+1,k+1} = a \omega^{n+1,k+1} + \rho_0 \end{array} \right\} \quad (6)$$

where n is the time step and k the iteration number. Note that (i) the flow equation depends on the fluid density and state variable ω at iteration k and (ii) Darcy's fluxes (step 2), and therefore the dispersion tensor, depend on head calculated at iteration $k + 1$ and density at iteration k (* symbol in the equations).

[12] Based on the Picard scheme, we suggest the following new algorithm:

$$\left. \begin{array}{l} \text{Step 1 : } c \frac{\omega^{n+1,k+1} - \omega^n}{\Delta t} + \mathbf{q}^{n+1,k} \cdot \nabla \omega^{n+1,k+1} - \nabla \cdot (\mathbf{D}^{n+1,k} \cdot \nabla \omega^{n+1,k+1}) = Q(\omega_s - \omega^{n+1,k+1}) \\ \text{Step 2 : } \rho^{n+1,k+1} = a \omega^{n+1,k+1} + \rho_0 \\ \text{Step 3 : } S \frac{h^{n+1,k+1} - h^n}{\Delta t} + \nabla \cdot \left(-\mathbf{K} \left(\nabla h^{n+1,k+1} + \frac{\rho^{n+1,k+1} - \rho_0}{\rho_0} \nabla z \right) \right) = Q \frac{c}{\rho} \frac{\partial \rho}{\partial \omega} \frac{\omega^{n+1,k+1} - \omega^n}{\Delta t} \\ \text{Step 4 : } \mathbf{q}^{n+1,k+1} = -\mathbf{K} \left(\nabla h^{n+1,k+1} + \frac{\rho^{n+1,k+1} - \rho_0}{\rho_0} \nabla z \right) \end{array} \right\} \quad (7)$$

The main difference lies in the flow equation and the expression of Darcy's fluxes. The transport equation is solved with velocities defined at the previous iteration. Because the flow equation is more dependent on the temperature or mass fraction than the transport equation on the heads (mass fraction or temperature variations in time create a sink/source term in the flow equation), this algorithm should reduce the number of iterations within one time step.

[13] For the first time step and the first iteration, the initial Darcy velocities are obtained by solving the flow equation, as for the standard algorithm.

[14] The same stopping criteria for the iterative schemes can be applied and therefore, no significant differences in accuracy should be found.

4. Numerical Experiments

[15] Both iterative schemes were implemented in the numerical model described in Ackerer et al. [1999] and Younès et al. [1999]. The implementation of the new scheme is easy, the calls of the routines have just to be switched. The efficiency of the suggested iterative scheme is illustrated by the simulation of strongly flow and transport problems in two and three dimensions. No significant differences in head and mass fraction distributions between already published results obtained with the standard scheme and the new scheme were found. Therefore, only the effects of the algorithms on the iterations are presented.

4.1. The Elder Problem

[16] The experimental study of Elder [1966] concerns the flow produced by heating the base of a porous layer. It is a free convection problem where fluid flow is driven purely by fluid density differences. It involves total density variations of 20% which makes this problem a strongly coupled flow case. The equivalent solute transport of this thermal problem corresponds to the salt water intrusion into uncontaminated aquifer by density-driven convection. This test case has been widely studied [Voss and Souza, 1987; Oldenburg and Pruess, 1995; Kolditz et al., 1998] (among others).

[17] The standard scheme requires 5041 iterations and a total CPU time of 289 seconds. The new scheme requires 3992 iterations and a total CPU time of 230 seconds without differences in the results (pressure and mass fraction). The stopping criteria used are the same for both calculations. They are based on the maximum change of the state variable between two iterations. The stopping criteria are equal to 10^{-7} for pressure and mass fraction. The new scheme reduces the maximum differences between two iterations for the flow calculation. These differences between both schemes remain small for the transport calculation (Figure 1).

4.2. The Saltpool Problem

[18] A 3D experiment, called the saltpool experiment, conducted by Oswald [1998] is used as a benchmark. A cube of $0,20 \times 0,20 \times 0,20 \text{ m}^3$ is filled with industrial glass beads. The porous medium is then saturated with pure water. The cube contains five openings (squares) of dimension $0,001 \times 0,001 \text{ m}^2$. The experiments were run in 3 steps:

- step 1: injection of the salt water in the middle of the bottom face of the cube.
- step 2: no injection or outflow.
- step 3: injection of pure water at one top vertex. Outflow occurs at the diagonal opposite top vertex.

[19] Simulated distributions of mass fraction in the cube, at the end of the step 1 ($t = 10 \text{ min}$), the end of the step 2 ($t = 45 \text{ min}$) and during the step 3 ($t = 63 \text{ min}$), are plotted in Figure 2.

[20] Oswald [1998] performed simulations of these experiments with a variety of codes to show the applicabil-

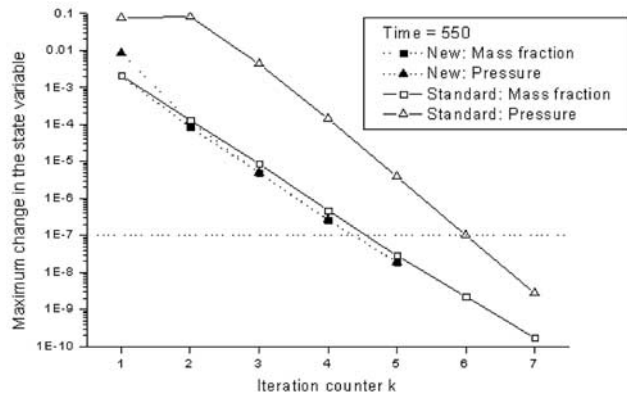


Figure 1. Maximum state variable differences between the standard and the new algorithm for the Elder problem.

ity of the experiments as a benchmark for verification of density-driven flow models. All these simulations gave quite different results and showed an overestimation of the maximum mass fraction compared to the experiments. Simulations done by *Ackerer et al.* [2000] and *Diersch and Kolditz* [2002] showed an underestimation of the maximum mass fraction. *Johannsen et al.* [2002] provided other simulations with a better match between computed and measured mass fractions. However, they only simulated the last step of the experiments. Therefore, initial conditions, especially the extension of the mixing zone, are additional fitting parameters.

[21] Same stopping criteria are used and the maximum admissible change in the variables between 2 iterations was fixed to 10^{-5} . The simulation of the experiments requires

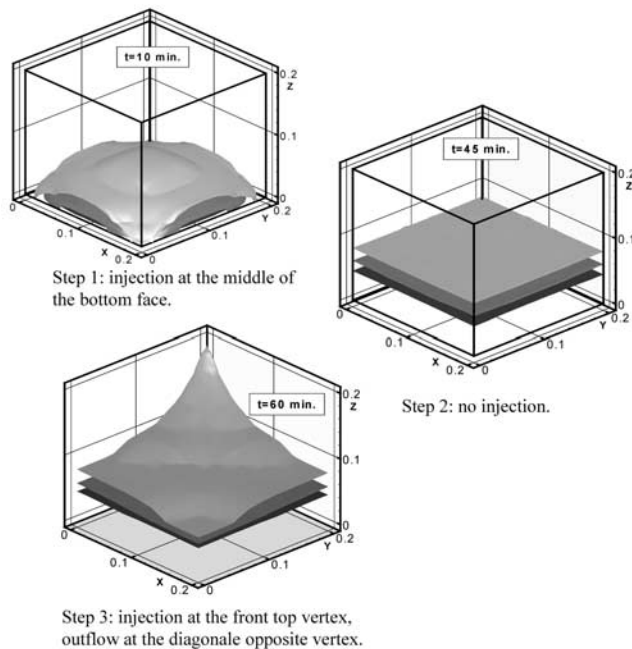


Figure 2. Distribution of mass fraction in the cube for the saltpool problem. (Iso-surface: 0.05, 0.5, 0.8. Inflow at $x = 20$ cm, $y = 0.0$ cm, $z = 20$ cm, outflow at $x = 0.0$ cm, $y = 20$ cm and $z = 20$ cm).

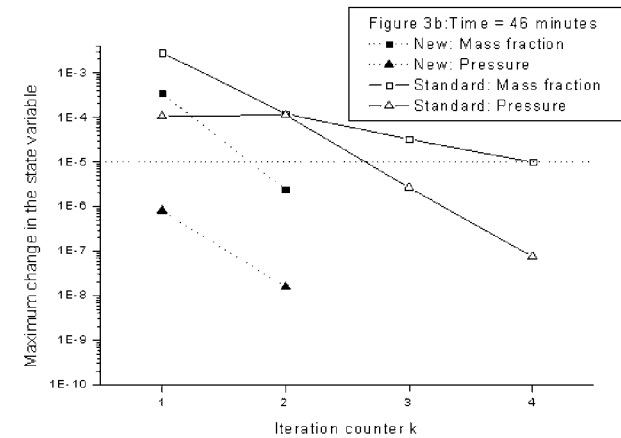
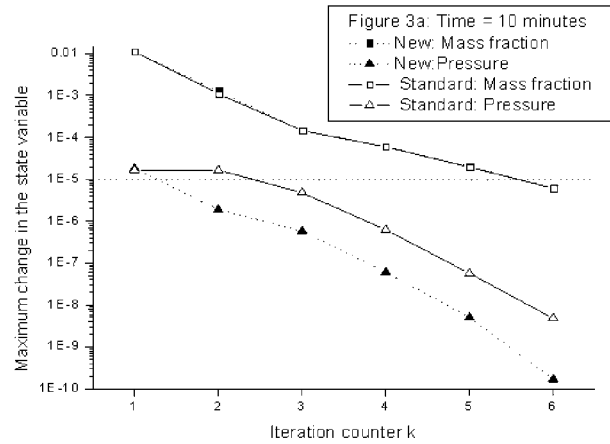


Figure 3. Maximum state variable differences between the standard and the new algorithm for the Saltpool benchmark at (a) 10 min and (b) 46 min.

9047 iterations and 43 hours of CPU time for the standard scheme and 6219 iterations and 30.5 hours of CPU time for the new scheme. The changes in the maximum differences between successive iterations within one time step are shown in Figure 3. As for the 2D test, the flow calculation is improved by the new algorithm. This can lead to a significant reduction of the number of iterations within one time step (Figure 3b).

5. Conclusions

[22] Modeling flow and heat or mass transport in porous medium requires to solve a strongly coupled system of partial differential equations. Adapted mathematical formulation and algorithm can reduce significantly the required CPU time without loss of accuracy.

[23] Based on the Picard scheme, we provided a new iterative coupling scheme, which consists in solving firstly the transport equation and, then, subsequently, the flow equation, on the contrary of the standard scheme. This can lead to a diminution of the number of iterations within one time step, and thus, a diminution of the CPU time. Taking the CPU time for the standard scheme as reference, the diminution of the CPU time was found about 20% for the two dimensional test case and about 30% for the three dimensional case. Results show that the new scheme

reduces the differences between the estimated variable used for the linearization (value of the variable at the previous iteration) and the computed variable essentially for the flow equation. Similar benefits in CPU time have been obtained for other test cases including field cases.

[24] This new algorithm is easy to implement and is not dependent on the numerical methods.

[25] **Acknowledgment.** We are grateful to the ‘ACI Globalisation des Ressources Informatiques et des Données’ for the financial support.

References

- Ackerer, P., A. Younès, and R. Mosé (1999), Modeling variable density flow and solute transport in porous medium: 1. Numerical model and verification, *Transp. Porous Media*, 35(3), 345–373.
- Ackerer, P., A. Younès, S. Oswald, K. Kinzelbach (2000), On modelling of density-driven flow: Calibration and reliability in groundwater modeling: Coping with uncertainty, in *Proceedings of the ModelCARE99 Conference Zurich*, edited by F. Stauffer et al., *IAHS Publ.*, 265, 377–384.
- Bear, J. (1972), *Dynamics of Fluids in Porous Media*, Elsevier Sci., New York.
- Diersch, H. J., and O. Kolditz (1998), Coupled groundwater flow and transport: 2. Thermoline and 3D convection systems, *Adv. Water Res.*, 21, 401–425.
- Diersch, H. J., and O. Kolditz (2002), Variable-density flow and transport in porous media: Approaches and challenges, *Adv. Water Res.*, 25, 899–944.
- Elder, J. W. (1966), Numerical experiments with a free convection in a vertical slot, *J. Fluid Mech.*, 24, 43–823.
- Hassanizadeh, S. M., and T. Leijnse (1988), On the modeling of brine transport in porous media, *Water Resour. Res.*, 24, 321–330.
- Holzbecher, E. (1998), *Modeling Density-Driven Flow in Porous Media*, Springer-Verlag, New York.
- Huyakorn, P., P. Anderson, J. Mercer, and H. White Jr. (1987), Saltwater intrusion in aquifers: Development and testing of a three-dimensional finite element model, *Water Resour. Res.*, 23, 293–312.
- Johannsen, K., W. Kinzelbach, S. Oswald, and G. Wittum (2002), The saltpool benchmark problem-numerical simulation of salt water upcoming in a porous medium, *Adv. Water Res.*, 25, 335–348.
- Kolditz, O., R. Ratke, H. J. Diersch, and W. Zielke (1998), Coupled groundwater flow and transport: 1. Verification of variable-density flow and transport models, *Adv. Water Resour.*, 21, 27–46.
- Oldenburg, C., and K. Pruess (1995), Dispersive transport dynamics in a strongly coupled groundwater-brine flow system, *Water Resour. Res.*, 31, 289–302.
- Oswald, S. (1998), Dichteströmungen in porösen Medien: Dreidimensionale Experimente und Modellierung, Ph.D. thesis, ETH Zürich.
- Oswald, S. E., and W. Kinzelbach (2004), Three-dimensional physical benchmark experiments to test variable-density flow models, *J. Hydrol.*, 290(1–2), 22–42, doi:10.1016/j.jhydrol.2003.11.037.
- Voss, C., and W. Souza (1987), Variable density flow and solute transport simulation of regional aquifers containing a narrow freshwater-saltwater transition zone, *Water Resour. Res.*, 23, 2097–2106.
- Younès, A. (2003), On modelling the multidimensional coupled fluid and heat or mass transport in porous media, *Int. J. Heat Mass Transfer*, 46, 367–379.
- Younès, A., P. Ackerer, and R. Mosé (1999), Modeling variable density flow and solute transport in porous medium: 2. Re-evaluation of the salt dome flow problem, *Transp. Porous Media*, 35(3), 375–394.

P. Ackerer, Institut de Mécanique des Fluides et des Solides, UMR 7507, 2 rue Boussingault, F-67000 Strasbourg, France. (ackerer@imfs.u-strasbg.fr)

M. Mancip, Projet Estime, INRIA Rocquencourt, BP 105, F-7153 Le Chesnay Cedex, France.

A. Younès, Laboratoire de Génie Industriel, Université de la Réunion, St. Denis, France.